

Estimation of Projection Effect of CMEs from the Onset Time of the Shock-Associated Type III Radio Burst

by

G. Michałek^{1,2}, N. Gopalswamy³ and S. Yashiro²

¹ Astronomical Observatory of Jagiellonian University, ul. Orla 171, 30-244 Kraków, Poland

e-mail: michalek@oa.uj.edu.pl

² Center for Solar and Space Weather, Catholic University of America, Washington, DC 20064

³ NASA Goddard Space Flight Center, Code 695, Greenbelt, MD 20771

Received October 27, 2004

ABSTRACT

We present a new possibility to estimate the projection effects on coronal mass ejection (CME) measurements. It is well known that coronagraphic observations of CMEs are subject to projection effects. Fortunately, the WIND/WAVES observations of type III radio bursts associated with shock waves are free from projection effects. We assume that (1) high energy electrons are produced at the shock front ahead of the CME, and (2) the radio burst starts when the shock reaches open field lines ($\approx 3 R_{\odot}$). In other words, the onset time of the radio burst corresponds to the time when the CME leading edge reaches $3 R_{\odot}$. The difference between the onset times of CMEs and radio bursts should be strongly correlated with the position of CMEs on the Sun. This correlation seems to be strongly dependent on solar activity. Using particular linear fits on the scatter plots, we can determine the source location of CMEs and tell how much the projection effect can really affect CME measurements.

Key words: *Sun: coronal mass ejections (CMEs) – Sun: radio radiation*

1. Introduction

Since 1995 the LASCO experiment on board of the SOHO satellite images the corona continuously with high sensitivity and dynamic range (Howard *et al.* 1997). In spite of major advantages over previous instruments, observations by the LASCO coronagraph are still affected by a projection effect especially for coronal mass ejections (CMEs) originating on the disk (Howard *et al.* 1982). Coronagraphic observations, recording photospheric photons scattered on electrons in solar corona, do not allow us to find the space properties of dynamic structures appearing above the Sun. Parameters describing properties of CMEs such as velocity,

acceleration, heliocentric distance and width are determined in the plane of the sky only. Coronal mass ejections originating from regions close to the central meridian of the Sun and directed toward the Earth can cause severe geomagnetic storms. These crucial parameters could be useful to define geoeffectiveness of CMEs. A definite correlation between the longitude of the solar source and speed of CMEs (Gopalswamy *et al.* 2000) confirmed the existence of a significant projection effect. Attempts made to estimate the projection effect based on the location of the solar source are based on *ad hoc* assumptions on parameters such as the width of CMEs (Sheeley *et al.* 1999, Leblanc and Dulk 2001). Recently, Michalek *et al.* (2003) and Xie *et al.* (2004) used a cone model for CMEs trying to determine the real parameters in describing full halo CMEs. In this paper, we attempt to correct it for the projection effect, based on radio bursts in the decameter-hectometric (DH) wavelength regime, observed by the RAD2 receiver of the WIND/WAVES experiment (Bougeret *et al.* 1995). The RAD2 receiver covers the decameter-hectometric (DH) frequency range 1.075–13.825 MHz, which corresponds to the transition region between the solar corona and interplanetary medium, *i.e.*, from $\approx 2 R_{\odot}$ to $20 R_{\odot}$. Interplanetary radio bursts associated with shocks (type II), electron beams (type III burst) and moving coronal structures (type IV burst) are observed in this domain. All these radio bursts are produced by non-thermal electrons. The fast-drift type III radio bursts appear when a beam of energetic electrons passes through the interplanetary plasma. Such a situation arises when energetic electrons produced by CME-driven shock waves enter open magnetic field structure. At heliocentric distances $> 2.5 R_{\odot}$ the solar wind begins to dominate and open magnetic field lines are seen in the interplanetary medium (IP). The local plasma frequency at these distances is typically about a few MHz, consistent with the onset of type III-like bursts associated with CME-driven shocks (Reiner *et al.* 1999, Bougeret *et al.* 1998). In the present paper we combine white light CME observations made by the LASCO coronagraph and radio burst observations of the WIND/WAVES experiment to estimate the projection effects. We assume that (1) high energy electrons are produced at the shock front ahead of CME, and (2) the type III-like radio burst starts when the shock reaches open field lines ($\approx 3 R_{\odot}$). In other words, the onset time of the type III-like radio burst corresponds to the time when the CME leading edge reaches $3 R_{\odot}$. The difference between onset times of CMEs and radio bursts should be strongly correlated with the position of CMEs on the Sun. We found this correlation to be significant with correlation coefficient, $R = 0.76 \pm 0.01$. We produced scatter plots of delay time vs. event longitude and showed that this correlation strongly depends on a solar activity phase.

2. Determination of Delay Time

We consider a sample of 60 type II burst events (covering a time period from April 1997 through July 2000) in the decameter-hectometric (DH) radio window

(1–14MHz). Gopalswamy *et al.* (2000) showed that all the DH type bursts are associated with large-scale CMEs. In a similar fashion, we identified the white light CMEs corresponding to each of these type II bursts. For each event we also identified the heliographic location based on the position of the $H\alpha$ flare or the position of the filament eruption. We obtained from LASCO observations height-time plots of CMEs (Yashiro *et al.* 2004) to extrapolate the estimated time, T_1 , when CMEs would reach in the plane of sky a heliocentric distance of $3 R_{\odot}$. To avoid acceleration effects, T_1 is estimated from measuring only four LASCO frames when the height of a CME is closest to $3 R_{\odot}$. Similarly, from the corresponding WAVES spacecraft dynamic spectra, we determine beginning time, T_2 , for the type III radio burst. We have to note, that the starting frequency of this radio burst should be in the vicinity of 7 MHz which corresponds to the heliocentric distance $\approx 3 R_{\odot}$. Of course, T_1 strongly depends on projection effects and should be delayed with respect to T_2 . The delay time, $\Delta T = T_1 - T_2$, should increase with decreasing longitude of CMEs. It is important to note that the time accuracy of both instruments is very good. Any errors which could affect determination of the delay time originate from the fitting procedure. The standard deviation error for the delay times in all figures are shown as bars. We have to mention that we consider delay time *vs.* solar longitude only. CMEs mostly originate very close to the solar equator (for the considered CMEs $|\text{latitude}| < 30^\circ$) and dependence of the delay time on latitude is assumed insignificant.

3. Results

The longitude constraint was placed on all events. In Fig. 1, the scatter plot shows a definite negative correlation (correlation coefficient $R = 0.76 \pm 0.01$). The solid line is the linear fit to the data points. It is clear that the correlation is significantly affected by velocity and width of individual events. With the same location on the Sun, faster and wider events should have smaller delay time. This seems to be confirmed by Fig. 2. In the two respective panels, we present scatter plots of delay time *vs.* event velocity for disk and limb events. The solid lines are the linear fits to data points. The velocity of disk events shows negative correlation with delay time. For limb events, which are free from projection effects, this correlation is poorer and the delay times are shorter in comparison with disk events. We need to remember that solar corona properties depend on the location above the disk and solar activity. By looking at different solar activity phases, the correlation coefficient may determine the location of the CME in the solar corona. In Fig. 3, the correlation between the delay time and longitude are given for events during the ascending (years 1997–1998) and the maximum phases of solar activity (years 1999–2000). The correlation coefficient increased for events during the ascending phase of solar activity ($R = 0.82 \pm 0.02$). The dashed lines are linear fits to the data points for the respective solar phases. The solid line in the bottom panel is

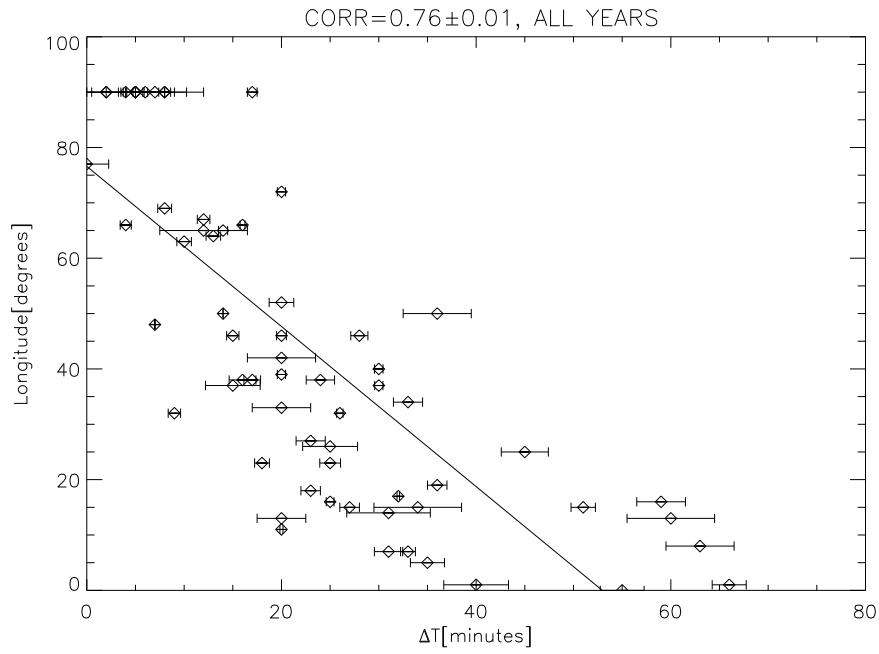


Fig. 1. Scatter plot of the delay time ($\Delta T = T_1 - T_2$) against event longitude (correlation coefficient = 0.76). The solid line is the linear fit to the data points.

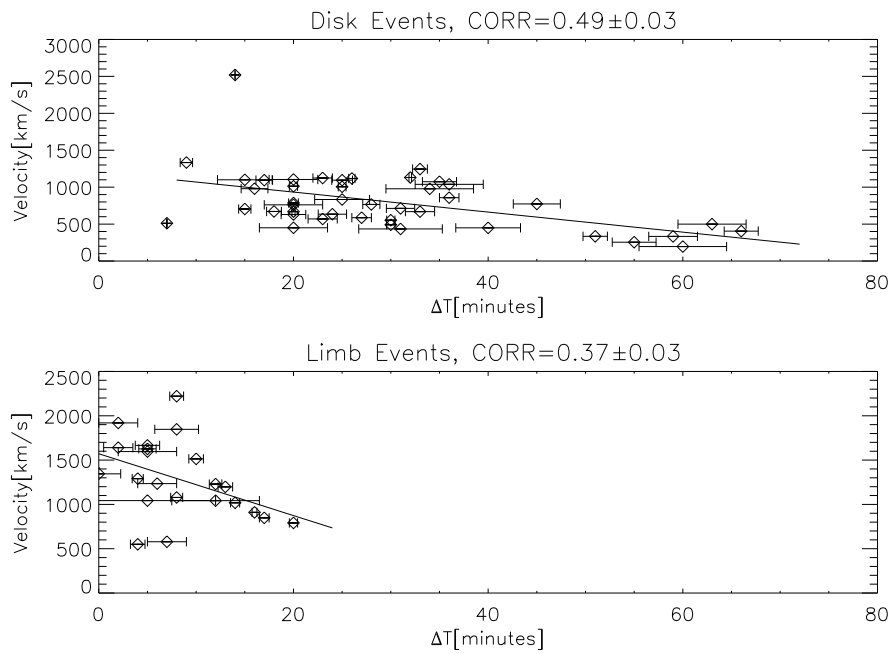


Fig. 2. Scatter plots of the delay time ($\Delta T = T_1 - T_2$) vs. event velocity. The solid lines are the linear fits to the data points. The *upper panel* is for disk event with longitude $< 60^\circ$. The *bottom panel* is for limb events with longitude $> 60^\circ$.

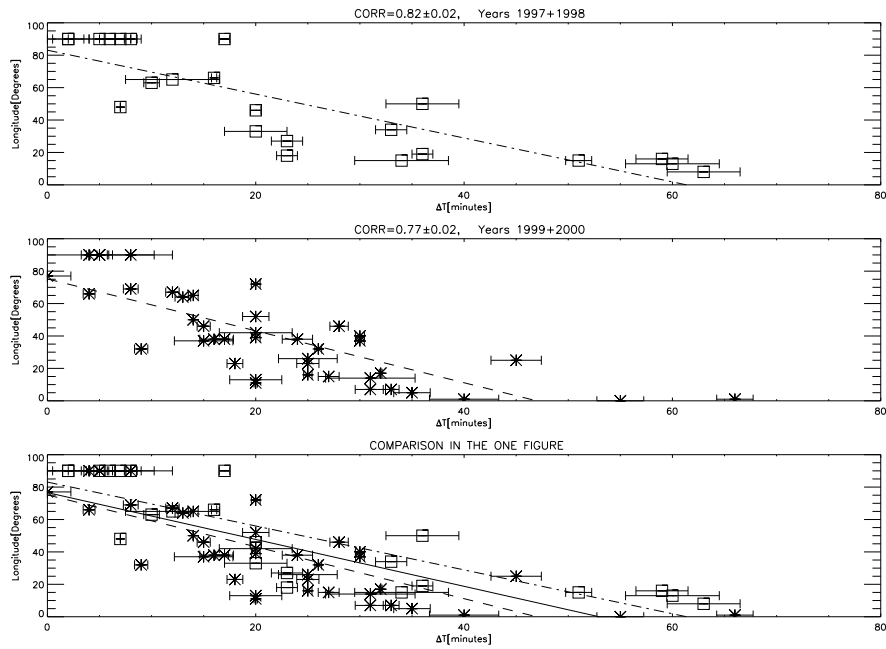


Fig. 3. In the respective panels we present the scatter plots of the delay time ($\Delta T = T_1 - T_2$) vs. event longitude during the ascending (1997–1998) and maximum phases of solar activity (1999–2000) as well as for the whole period (1997–2000). The dashed lines are linear fits to the data points. The solid line in the *bottom panel* is for comparison only and shows linear fit to all events from our sample.

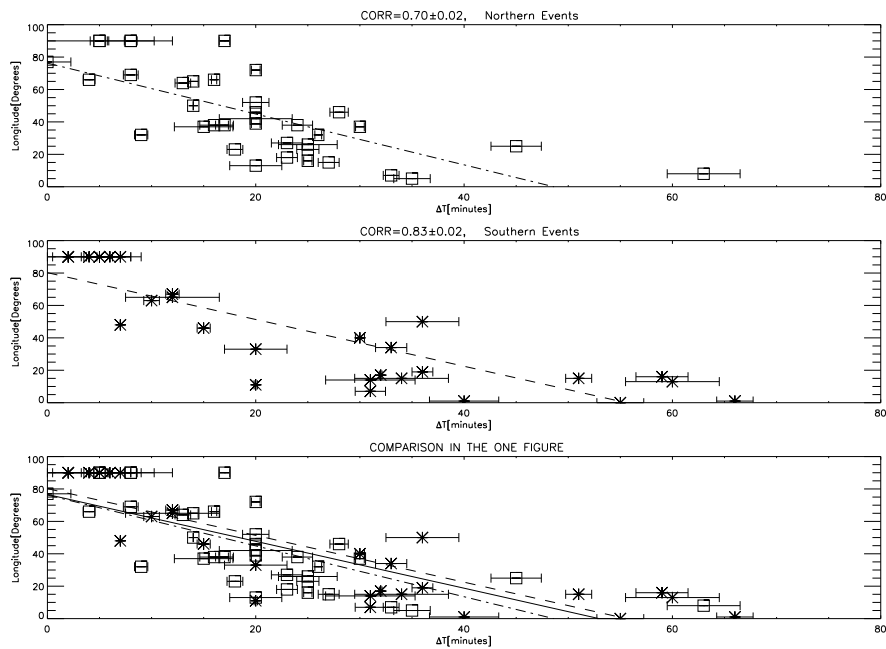


Fig. 4. In the respective panels we present the scatter plots of the delay time ($\Delta T = T_1 - T_2$) vs. event longitude for northern, southern and entire solar heliosphere. The dashed lines are linear fits to the data points. The solid line in the *bottom panel* is for comparison only and shows linear fit to all events from our sample.

for comparison only and shows the linear fit to all events. The inclination of the linear fit during maximum solar activity is steeper in comparison with the slope of the linear fit during the ascending phase of solar activity. This means that during the maximum solar activity closed coronal magnetic field lines are open at higher heliocentric distances. Thus, during the maximum solar activity the delay times are smaller. In Fig. 4 scatter plots of the delay time vs. longitude for events appearing at the northern and southern heliosphere are presented. Respective dashed lines represent linear fits to the data points. Now, the correlation coefficient is larger for southern events ($R = 0.83 \pm 0.02$) in comparison with northern ($R = 0.70 \pm 0.02$) events. This suggests that the solar corona is more ordered in the northern hemisphere. The slopes of the linear fits (compared in the lower panel) for both hemispheres are very similar. We can see similar differences between the eastern and western hemispheres. In Fig. 5 we present the scatter plots of the delay time vs.

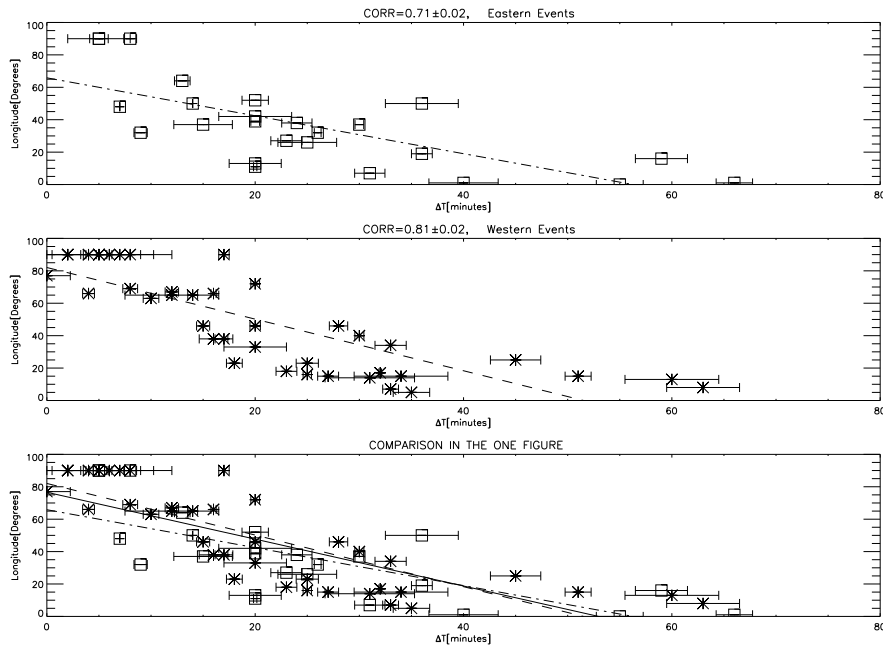


Fig. 5. In the respective panels we present the scatter plots of the delay time ($\Delta T = T_1 - T_2$) vs. event longitude for eastern, western and entire solar heliosphere. The dashed lines are linear fits to the data points. The solid line in the *bottom panel* is for comparison only and shows linear fit to all events from our sample.

longitude for events localized in the eastern and western hemispheres. Finally for comparison, both scatter plots are shown in one panel. Now, events originating in the western hemisphere have a higher correlation ($R = 0.81 \pm 0.02$) in comparison with events located in the eastern hemisphere ($R = 0.71 \pm 0.02$). The slope of the linear fits is similar for the southern and northern hemisphere. The results presented in Figs. 3–5 show that the correlation between the delay time and longitude is strongly affected by the dynamics of the solar corona. It depends largely on the

solar activity phase. On the other hand, we do not observe significant changes in the inclination of the slope when we consider events originating in different hemispheres.

4. Summary

In the present paper, comparing data received from radio observation and LASCO coronagraph, we tried to determine the correlation between the delay time and longitude of CMEs. We found for all events a significant correlation ($R = 0.76 \pm 0.01$) between the onset times of CMEs and radio bursts with the longitude of CMEs on the Sun. Unfortunately, due to different effects data points were significantly scattered around the linear fits. We showed that the correlation is affected by velocity and width of individual CME events and the evolution of coronal magnetic field lines at different solar activity phases. The correlation could significantly change during solar cycles. This means that open magnetic field lines do not always appear at a heliocentric distance of $3 R_{\odot}$. To improve results, we considered CMEs appearing in different solar activity phases. We found that during maximum solar activity closed coronal magnetic field lines are stronger and open at higher heliocentric distances in the IP making the delay times smaller. We demonstrated that linear fits do not significantly depend on what hemisphere CMEs originate.

It is important to note that solar corona is an inhomogeneous structure changing in space and time. The assumption that magnetic field lines open in the IP at heliocentric distance $3 R_{\odot}$ is only an approximation. This distance is variable and depends on a particular event. This can be proven by considering limb events (longitude 90°). An ideal situation for these particular events is that the delay time should be equal zero. For events in our sample delay times for such CMEs could be equal even to 20 minutes. In spite of very simple assumption good results (correlation coefficients are significant) were obtained. The presented linear fits can be used to estimate the projection effect for a particular CME when the delay time, ΔT , is determined.

Acknowledgements. In this paper we used data from SOHO/LASCO CME catalog. This CME catalog is generated and maintained by the Center for Solar Physics and Space Weather, The Catholic University of America in cooperation with the Naval Research Laboratory and NASA. SOHO is a project of international cooperation between ESA and NASA.

Work done by Grzegorz Michalek was partly supported by the KBN grant PB 0357/P04/2003/25.

REFERENCES

- Bougeret, J.,-L., *et al.* 1995, *Space Sci. Rev.*, **71**, 231.
Bougeret, J.,-L., *et al.* 1998, *Geophys. Res. Lett.*, **25**, 2513.

- Gopalswamy, N., *et al.* 2000, *Geophys. Res. Lett.*, **27**, 1427.
- Gopalswamy, N., *et al.* 2001, *J. Geophys. Res.*, **106**, 2929.
- Howard, R.A., *et al.* 1982, *Astrophys. J. Letters*, **263**, L101.
- Howard, R.A., *et al.* 1997, "Observations of CMEs from SOHO/LASCO", *Geophysical Monograph* 99: Coronal mass ejections, Ed. N. Crooker, AGU, p 17.
- Leblanc, Y., and Dulk, G.A. 2001, *J. Geophys. Res.*, **106**, 25301.
- Michalek, G., *et al.* 2003, *Astrophys. J.*, **584**, 472.
- Rainer, M.J., and Kaiser, M.L. 1999, *Geophys. Res. Lett.*, **26**, 397.
- Sheeley, N.R., Jr., Walters, J.H., Wang, Y.-M., and Howard, R.A. 1999, *J. Geophys. Res.*, **104**, 24739.
- Xie, H., *et al.* 2004, *J. Geophys. Res.*, **109**, A03109.
- Yashiro, S., *et al.* 2004, *J. Geophys. Res.*, **109**, A07105.